ELSEVIER ELSEVIER

Contents lists available at ScienceDirect

Earth and Planetary Science Letters

www.elsevier.com/locate/epsl



Helium and oxygen isotopic variations in the Iceland plume source controlled by entrainment of recycled oceanic lithosphere



Maja B. Rasmussen ^{a,*}, Sæmundur A. Halldórsson ^a, Matthew G. Jackson ^b, Ilya N. Bindeman ^c, Martin J. Whitehouse ^d

- ^a Nordic Volcanological Center, Institute of Earth Sciences, University of Iceland, Askja, Sturlugata 7, 102 Reykjavik, Iceland
- ^b Department of Earth Science, University of California Santa Barbara, 552 University Road, Santa Barbara, 93106-9630, USA
- ^c Department of Earth Sciences, University of Oregon, 1255 E 13th Ave, Eugene, OR 97403, USA
- d Department of Geosciences, Swedish Museum of Natural History, Box 50007, SE-104 05 Stockholm, Sweden

ARTICLE INFO

Article history: Received 13 June 2021 Received in revised form 3 June 2022 Accepted 21 June 2022 Available online 20 July 2022 Editor: R. Dasgupta

Keywords: oxygen isotopes helium isotopes olivine Iceland Plateau mantle heterogeneity

ABSTRACT

Icelandic basalts have low oxygen isotope (δ^{18} O) values compared to other ocean island localities. While this observation is often ascribed to the assimilation of low- $\delta^{18}O$ crust, a low- $\delta^{18}O$ mantle beneath Iceland has also been suggested. To discern crustal from mantle-derived signals, high-quality in-situ and bulk crystal δ^{18} O measurements have been obtained from olivine crystals covering 16 Ma of activity at the Iceland hotspot. The results are combined with olivine (ol) major, minor and trace element chemistry. Relationships between $\delta^{18}O_{ol}$ and indicators of melt evolution do not support a singular process responsible for lowering of $\delta^{18}O$ values. However, correlations are observed between $\delta^{18}O_{ol}$ values and indicators of crustal processes. Such patterns are used to filter out data that are likely to reflect effects from crustal assimilation to highlight $\delta^{18}O_{ol}$ values indicative of source-derived variability only. Although filtered, the dataset reveals, that $\delta^{18}O_{ol}$ values, significantly lower than the canonical depleted upper mantle value, are derived from the Iceland mantle. Coupled $\delta^{18}O_{ol}$ and ${}^{3}He/{}^{4}He_{ol}$ measurements done on olivine crystals from the same samples demonstrate that low- δ^{18} O components (down to δ^{18} O_{olivine} = 4.2\%) are a trait of the modern Iceland plume and that low- δ^{18} O and low- 3 He/ 4 He components have become more apparent in the hotspot products since 60 Ma. Olivine chemistry characteristics suggest that this low- δ^{18} O component is best sampled in melts that reflect contributions from pyroxenitic mantle lithologies, likely related to the recycling of oceanic lithosphere within the plume. An increase in plume flux, as traced by increasing plume temperatures and plume buoyancy after 35 Ma, led to enhanced entrainment of lower mantle material carrying recycled low- δ^{18} O oceanic lithosphere. Such material has become more apparent with time as is reflected in source-derived low-6180 and high 3He/4He values in olivine from the modern Iceland plume. Moreover, the coincidence of the Iceland plume-head and the North Atlantic Rift at from \sim 25 Ma likely assisted and further promoted enhanced plume-melting. Thus, the combination of changes in mantle upwelling and tectonic reorganisation of the North Atlantic led to the introduction of recycled oceanic lithosphere into the Iceland plume and the formation of the Iceland Plateau ~25 Ma.

© 2022 Elsevier B.V. All rights reserved.

1. Introduction

Oxygen is the most abundant element in the silicate Earth, and its isotopes are widely used as fingerprints of relative mantle and crustal contributions in melts. Deviations from the canonical upper mantle δ^{18} O (where δ^{18} O is defined as the difference

E-mail addresses: maja@hi.is, mr@ign.ku.dk (M.B. Rasmussen).

between sample and standard $^{18}\text{O}/^{16}\text{O}$ in %0) are widespread in ocean island basalts and have been associated with chemical heterogeneities in their source regions (Workman et al., 2008; Day and Hilton, 2011). Iceland is the largest subaerial expression of an oceanic ridge segment, which is due to the juxtaposition of a high-buoyancy, deep-seated mantle plume beneath the North Atlantic Rift. Basalts from the individual rift and off-rift systems constituting the volcanically active regions in Iceland, referred to as the neovolcanic zones, have unique geochemical characteristics (Harðardóttir et al., 2018; Kokfelt et al., 2006). Moreover, δ^{18} O values of Icelandic basalts are notably low compared to the depleted

^{*} Corresponding author at: Department of Geosciences and Natural Resource Management, University of Copenhagen, Øster Voldgade 10, 1350 Copenhagen, Denmark

MORB mantle (DMM) with $\delta^{18} O_{ol}$ of 5.1 \pm 0.3‰ (Eiler, 2001). Two prevailing hypotheses have been considered to account for this: shallow assimilation of low- $\delta^{18} O$ crust, or heterogeneity within the mantle source, possibly inherited from low- $\delta^{18} O$ oceanic crust recycled from ancient subduction zones (e.g., Thirlwall et al., 2006).

Meteoric water in Iceland has δ^{18} O values down to -14% (Sveinbjörnsdóttir et al., 2020), caused by the high-latitude location of the island. Interaction between this water and the Icelandic crust has resulted in crustal δ^{18} O values down to -10.5% measured in hydrothermally altered basalt from Krafla (Hattori and Muehlenbachs, 1982; Zakharov et al., 2019). Assimilation of this material into ascending melts could lower the δ^{18} O of this melt, and this process has indeed caused δ^{18} O_{melt} values down to 3% in large-volume tholeites basalts from the active rift zones (e.g., Bindeman et al., 2008; Halldórsson et al., 2018).

Despite evidence for overprinting of mantle-derived $\delta^{18}O_{ol}$ values in such basalts (Bindeman et al., 2008), previous studies have suggested the presence of a low- $\delta^{18}O$ component in the Iceland mantle (Kokfelt et al., 2006; Macpherson et al., 2005; Thirlwall et al., 2006; Winpenny and Maclennan, 2014) characterised by δ^{18} O values >1\% below that of DMM. However, most of these studies are based on bulk olivine analyses (Kokfelt et al., 2006; Macpherson et al., 2005; Thirlwall et al., 2006) which do not resolve intra-crystal variations caused by growth of olivine in equilibrium with an evolving melt affected by assimilation processes (Bindeman et al., 2008). Indeed, bulk olivine analyses have previously been shown to skew results towards crustal modified δ^{18} O values rather than primary mantle-derived values, because of the volume dominance of the low- $\delta^{18}{\rm O}$ rims. Thus, bulk analyses alone create difficulties when distinguishing between primary source-derived and secondary process-derived δ^{18} O values, and a combination of spatially resolved in-situ ('spot') and high-precision bulk techniques should be used to distinguish δ^{18} O values representative of the Icelandic mantle (Bindeman et al., 2008).

This study attempts to determine if low- δ^{18} O values are present in the mantle beneath Iceland by combining previously determined ${}^3\text{He}/{}^4\text{He}$ and compositional analyses (minor and trace elements) in olivine (ol), with new $\delta^{18}\text{O}_{ol}$ measurements of the same olivine populations. To circumvent material likely to be affected by interaction with low- $\delta^{18}\text{O}$ crust, only high-forsterite (Fo = Mg/(Mg + Fe) mol%) olivines are targeted, as olivine is one of the first phases to precipitate from a mantle-derived melt prior to significant crustal assimilation.

2. Sample selection and prior work

This study presents in-situ Secondary Ion Mass Spectrometry (SIMS, high spatial resolution) and single- and bulk crystal laser fluorination (LF, high-precision) δ^{18} O analyses of high-forsterite olivines (Fo₈₀₋₉₁) from across Iceland. The sample suite consists of olivine separates (listed in the data supplement T1) from 64 primitive lavas covering the active (neovolcanic <1 Ma) rift and flank zones along with older Quaternary and Tertiary (1-16 Ma) units (Fig. 1). Most of these (51 samples) were previously analysed for their minor- and trace element systematics (in-situ) and ³He/⁴He_{ol} values (Rasmussen et al., 2020; Harðardóttir et al., 2018), and show the largest ³He/⁴He range reported for any oceanic island (from 6.7 to 47.8R_A, where $R_A = air^3 He/^4 He$, Harðardóttir et al., 2018). Rasmussen et al. (2020) found that minor (e.g., Ni, Ca and Mn) and trace (e.g., Zn, Ga and Sc) element variations in the olivines studied here record the presence of hybrid pyroxenitic (olivinepoor) components - likely representing the presence of recycled oceanic crust in the Iceland mantle - which are best sampled in South Iceland. This geochemical signature coincides with a plumederived ³He/⁴He fingerprint, indicating that the lithological heterogeneity present in the Icelandic mantle is a trait of the upwelling

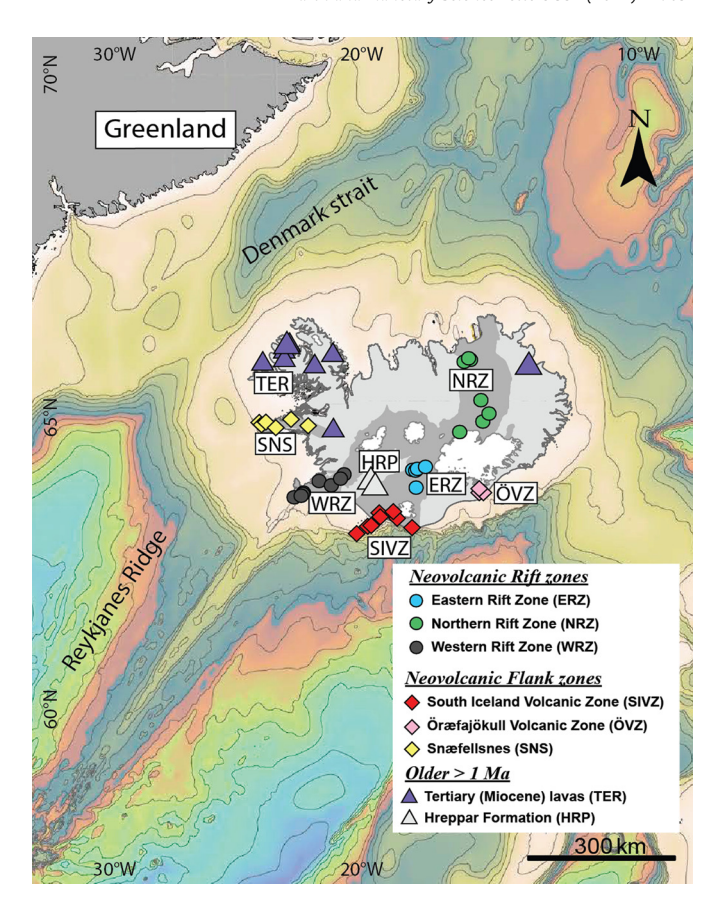


Fig. 1. Projection of sample localities and volcanic zones on a GEBCO-bathymetric map displaying the extent of the Iceland Plateau and the V-shaped ridges along the Reykjanes Ridge. Sample locations and zone abbreviations are identical to the divisions used in Rasmussen et al. (2020) and used throughout this study (data supplement T1). ERZ (Eastern Rift Zone), WRZ (Western Rift Zone) and NRZ (Northern Rift Zone) compromise the current rift axes. SIVZ (South Iceland Volcanic Zone) is a flank zone propagating from the southern tip of ERZ, while SNS (Snæfellsnes) and ÖVZ (Öræfajökull Volcanic Zone) are flank zones with alkalic to transitional magma products. TER covers Tertiary lavas, mostly from the West Fjords, while HRP (Hreppar formation) represents an isolated region with Plio-Pleistocene aged rocks, located between the WRZ and ERZ. The bathymetric map is generated using GMT software (Wessel and Smith, 1991). (For interpretation of the colours in the figure(s), the reader is referred to the web version of this article.)

plume. Thus, the extensive dataset collected on the same set of crystals presents a unique opportunity to identify primary versus secondary controls on the origin of the low- δ^{18} O signature predominating most Icelandic basalts.

The data presented here are classified according to the volcanic regions defined in Fig. 1 where ERZ (Eastern Rift Zone), WRZ (Western Rift Zone) and NRZ (Northern Rift Zone) constitutes the current rift axis. SIVZ (South Iceland Volcanic Zone) is a flank zone propagating southward from ERZ where transitional and alkalic magmas prevail similarly to products from the two other flank zones, ÖVZ (Öræfajökull Volcanic Zone) and SNS (Snæfellsnes). TER represents olivine from Tertiary lavas from the West and East fjords, while HRP (Hreppar formation) represents an isolated region with Plio-Pleistocene aged rocks, located between the WRZ and ERZ (Fig. 1).

3. Methods

3.1. Secondary ion mass spectrometry

In-situ δ^{18} O values of olivine (51 olivine samples, 91 crystals and 210 individual analyses, listed in data supplement T2), covering the entirety of the exposed modern Iceland (Holocene-

Miocene), were measured using a CAMECA IMS1280 Secondary Ion Mass Spectrometry (SIMS) instrument at the NordSIMS facility at the Swedish Museum of Natural History over three sessions. Prior to the SIMS measurements, the exact same spots were analysed by high-precision Electron Microprobe Probe Analyser (EMPA); for the complete dataset and analytical details see Rasmussen et al. (2020). Based on the major and minor element variability (Fig. S2), one to three grains were analysed for every sample with a minimum of two point-measurements per crystal (data supplement T2). Between EMPA and SIMS analysis, the carbon coating used for EMPA measurements was replaced by gold coating (30 nm) following repolishing with fine (1 μ m) grit. The oxygen isotopic values presented in this study are reported relative to V-SMOW in standard delta notation (δ) following equation (1):

$$\delta = \left[\frac{\frac{^{18}O}{^{16}O \text{ sample}}}{\frac{^{18}O}{^{16}O \text{ V-SMOW}}} - 1 \right] \cdot 1000 \tag{1}$$

A $^{133}\text{Cs+}$ primary beam with an incident energy of 20 keV and current of 2.5 nA was used to sputter secondary ions from the olivine. A small raster (10 μm) was used throughout the analysis to homogenise the critically focused beam and a low-energy normal incidence electron gun minimised sample charging. Measurement of secondary ions was performed at a mass resolution of 2500 (M/ ΔM) using multicollection on Faraday detectors connected to low-noise amplifiers housed in a thermally stabilised, evacuated chamber. The magnetic field was locked with high precision using an NMR field sensor. During the fully automated analytical sessions, reference analyses were carried out regularly following the analyses of six unknowns. Each individual analysis comprised a pre-sputter to remove the Au coat, followed by beam centring, and then 64 seconds of data acquisition.

Corrections for instrumental mass fractionation were made using San Carlos olivine, with Fo $_{90.6}$ (determined by EMPA). Importantly, this San Carlos standard has a δ^{18} O $_{ol}$ value of 5.25%, (supplement 1.2) determined by laser fluorination, and is thus the same composition as the San Carlos standards used by most other labs (e.g., Bindeman et al., 2008, Eiler et al., 1995). Instrumental mass fractionation from compositional changes was neglected as all crystals analysed were above Fo $_{80}$ (Isa et al., 2017). The standard deviation of the San Carlos δ^{18} O $_{ol}$ value varied slightly between the three sessions (see supplement 1.2). Thus, the instrumental error (1SD) of $\pm 0.17\%$ reflects an average instrumental error based on the three sessions. Each individual measurement was drift corrected based on regularly spaced standard measurements.

3.2. Laser fluorination

A subset of 20 olivine samples (53 analyses, listed in data supplement T3) from NW-Iceland (Vestfirðir), SIVZ, NRZ and ERZ were selected for oxygen isotopic analyses by laser fluorination (LF) in the Stable Isotope Laboratory at the University of Oregon. Note, that seven samples were analysed by both SIMS and LF (see data supplement T4). The LF analyses were carried out over four analytical sessions. All samples have two to five replicate δ^{18} O measurements, where different olivines were selected from a sample for each replicate analysis (data supplement T3). The forsterite composition for these samples were determined by EMPA (details in supplement 1.2).

Olivine crystals from each sample, some previously crushed to sizes of 500-850 μ m, were hand-picked and care was taken to avoid crystals with visible surface alteration, adhering groundmass, or crystals/melt inclusions. As indicated in T3 (data supplement), most $\delta^{18}O_{01}$ measurements consisted of multiple (\geq 4)

crystals being pooled for a single measurement, but some analyses consisted of a single crystal. Total olivine masses analysed ranged from 0.80-2.11 mg. Prior to analysis, some samples from Vestfirðir were leached in \sim 20% HF acid at room temperature for 10-30min to remove any alteration products or hourglass melt inclusions not visible under binocular microscope. Methods for the oxygen isotopic analyses of olivines follow Bindeman et al. (2008). Olivines were reacted with BrF₅ to release oxygen, and a 35 W CO₂ laser was used. Gas purification followed a cryogenic method using liquid N2, and a Hg-diffusion pump was used to eliminate any remaining F₂ from the fluorination process. Platinum-graphite was used to convert oxygen to CO₂ for analysis on a MAT253 mass spectrometer. Yields were measured using a baratron gauge and ranged from 12.63 to 13.8 μ mols O₂/mg. San Carlos olivine (δ^{18} O = 5.25\%), Gore Mt Garnet (UWG2, δ^{18} O = 5.80\%), [Valley et al., 1995]), and the University of Oregon Garnet (UOG, $\delta^{18}O = 6.52\%$) were used as standards. The data is reported relative to San Carlos Olivine (SCO = 5.25%) and precision of the measurements is estimated by concurrently running SCO along with the unknowns and recording the variability of this standard. This results in a precision of $\pm 0.07\%$ (1SD) or better based on four standards measurements.

4. Results

4.1. Oxygen isotope values of olivine crystals ($\delta^{18}O_{ol}$)

The SIMS results reveal limited intra-crystal variability (Fig. S1) but collectively display a variation in $\delta^{18} O_{ol}$ of $\sim\!3\%$ across Iceland (Fig. 2, data supplement T2). Olivine from the older formations (Miocene Tertiary lavas [TER] and Plio-Pleistocene Hreppar Formation [HRP]) cover almost the same range (5.6-3.3%) as the younger (<1 Ma) neovolcanic samples (6.1-2.8%). Similarly, the LF-derived $\delta^{18} O_{ol}$ record a comparable range in the TER samples (5.3-3.7%) and the neovolcanic samples (5.3-3.9%, supplement 1.3). Thus, LF and SIMS-derived data are overall in good agreement, recording $\delta^{18} O_{ol}$ values mostly below expected DMM values (5.1±0.3%, Fig. 2), consistent with a low- $\delta^{18} O_{ol}$ anomaly previously observed in Icelandic basalts (Bindeman et al., 2008; Macpherson et al., 2005; Thirlwall et al., 2006; Winpenny and Maclennan, 2014). A more detailed comparison of the datasets is available in Supplement 1.3.

4.2. Relationship between $\delta^{18}O_{ol}$ and minor and trace elements

The Fo, Mn and Zn content for the olivines analysed here were published by Rasmussen et al. (2020) and measured on the same spots and crystals as the new $\delta^{18}O_{ol}$ values. Overall, the rift-related samples extend to lower $\delta^{18}O_{ol}$ than the flank-related samples at a given Fo value or Mn and Zn content (Fig. 2). Moreover, no clear overall correlation is observed between $\delta^{18}O_{ol}$ and Fo values, which represents the effect of fractional crystallisation and evolving melt compositions. However, a lowering of $\delta^{18}O_{ol}$ is associated with a lowering of Fo values for some NRZ samples (Fig. 2a) from $\delta^{18} O_{ol}$ values just above 4% at Fo₉₀ to $\delta^{18} O_{ol}$ values around 3%at Fo₈₈. A similar pattern is observed when comparing δ^{18} O_{ol} values with the same-spot measured Mn (Fig. 2b) and Zn (Fig. 2c) likely highlighting similar effects resulting from melt evolution. Indeed, some NRZ olivines also display an increase in Mn contents with a lowering in $\delta^{18}O_{ol}$ corresponding to the pattern observed for Fo values (Fig. 2b), again highlighting the complex origin of the $\delta^{18}O_{ol}$ variation observed here.

4.3. Relationship between $\delta^{18}O_{ol}$ and element ratios

Minor and trace element ratios (e.g., Mn/Fe or Mn/Zn) have previously been determined for the olivine analysed. Relating Mn/Fe

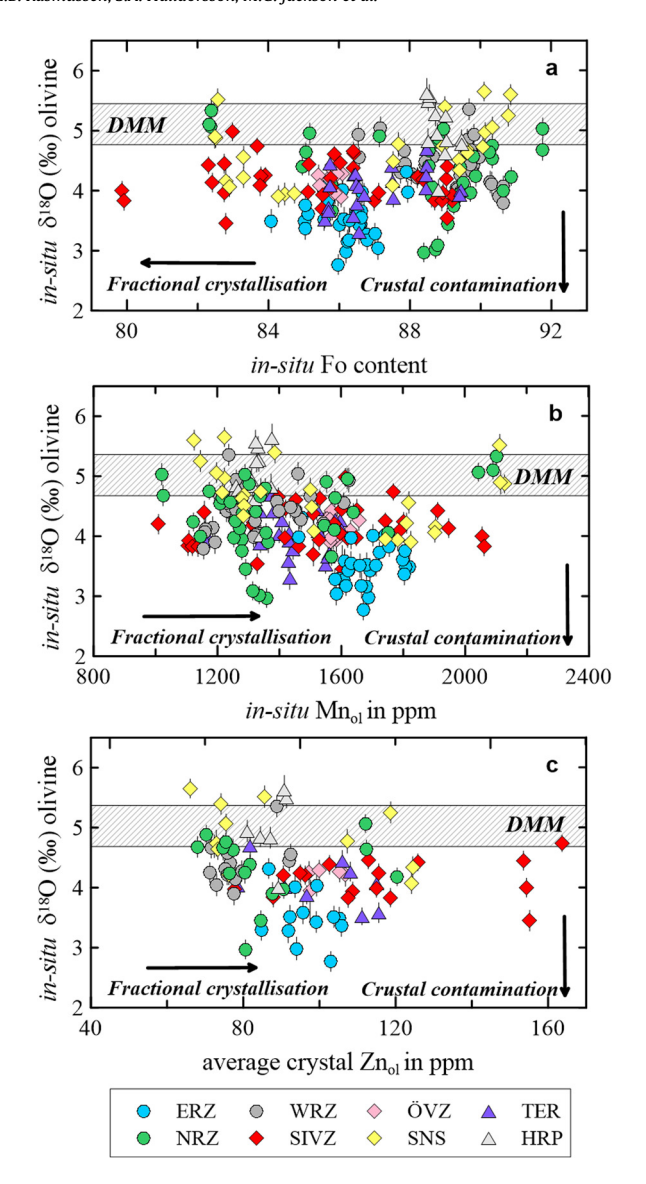


Fig. 2. δ^{18} O systematics of Icelandic olivine. a-c, Rift zone olivine extend to lower δ^{18} O_{ol} than the flank zone olivines. a) No clear correlation between Fo values and δ^{18} O_{ol} suggests that the in-situ δ^{18} O values observed are primary. b) A similar image is observed when relating δ^{18} O_{ol} values to Mn and Zn (in ppm) where no correlation is observed, highlighting lack of change in δ^{18} O_{ol} with melt evolution which often follows crustal assimilation. The major and minor element concentrations were measured on the same spots, and the trace element concentrations are based on crystal average from three point measurements on the same crystals as the δ^{18} O_{ol} measurements and can therefore be directly related. The crossed field represents the δ^{18} O of mantle-derived olivine from Eiler (2001). The errors associated with each data point correspond to the instrumental error (1SD).

with the newly acquired $\delta^{18} O_{ol}$ values presents two data trends: i) lowering $\delta^{18} O_{ol}$ values along with a lowering in Mn/Fe, especially evident in olivines from SIVZ, and ii) a trend with nearconstant Mn/Fe ratios but highly variable $\delta^{18} O_{ol}$ values (Fig. 3a). As such, the entire $\delta^{18} O_{ol}$ variation measured in Icelandic olivines is represented at a near-constant Mn/Fe value of approximately 1.6 (Fig. 3a). This is especially clear in olivines from ERZ which have near-uniform 100Mn/Fe $_{ol}$ values (between 1.57-1.64) but highly variable $\delta^{18} O$ values (between 2.77-4.32%). Olivines from the WRZ cluster around a $\delta^{18} O_{ol}$ value of 4.3% at 100Mn/Fe \sim 1.6, while NRZ olivines reveal highly heterogeneous $\delta^{18} O$ and 100Mn/Fe values (Fig. 3a). The TER, SIVZ and ÖVZ olivine all trend towards lower Mn/Fe values along with $\delta^{18} O_{ol}$ values mostly between 3.5-4.6% (Fig. 3a). A very similar pattern is observed when plotting Mn/Zn with $\delta^{18} O_{ol}$ (Fig. 3b).

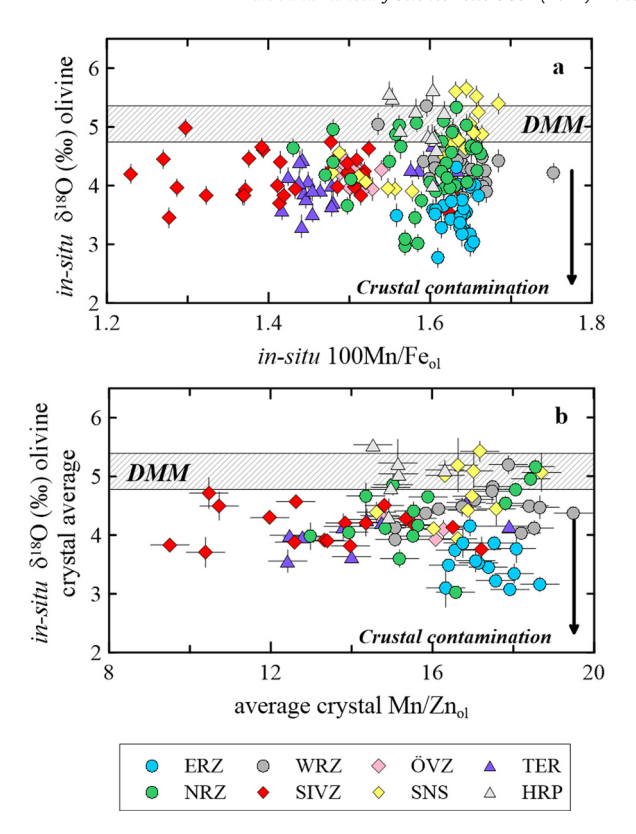


Fig. 3. Minor element ratios and $\delta^{18}O_{ol}$. a-b, As Mn/Fe (100*Mn/Fe) and Mn/Zn are corrected for fractional cystallisation and therefore unaffected by crustal processes (Rasmussen et al., 2020; Howarth and Harris, 2017; Sobolev et al., 2007), any correlation between Mn/Fe, Mn/Zn and $\delta^{18}O_{ol}$ suggests a source-control on the $\delta^{18}O_{ol}$. However, the variations in $\delta^{18}O_{ol}$ along a constant Mn/Fe and Mn/Zn suggest that some crustal assimilation also plays a role. This is observed especially in olivine from ERZ but also part of NRZ. The crossed field represents the $\delta^{18}O$ of mantle-derived olivine from Eiler (2001). The errors associated with each data point correspond to the instrumental error (1SD).

5. Discussion

5.1. Identifying secondary (crustal) controls on δ^{18} O values in Iceland

5.1.1. Melt evolution

Iceland's subaerial location at high latitudes results in low- δ^{18} O meteoric water (down to -14‰, Sveinbjörnsdóttir et al., 2020). The interaction of such waters with the Icelandic crust has been shown to result in subsurface hydrothermally altered basalts and hydrated subglacial basalts (hyaloclastites) with δ^{18} O_{bulk} values down to -10.5‰ (Hattori and Muehlenbachs, 1982; Zakharov et al., 2019). However, the bulk Icelandic crust is usually assigned an overall δ^{18} O composition between 0-2‰ (e.g., Bindeman et al., 2008; Macpherson et al., 2005; Gautason and Muehlenbachs, 1998; Eiler et al., 2000; Bindeman et al., 2012). This range of crustal δ^{18} O values is supported by direct sampling of the crust, such as drill cores from Reyðarfjördur (Eastern Iceland) and Reykjavik (Southwest Iceland) that were characterised by δ^{18} O values of 2‰ at depths down to 3 km (Hattori and Muehlenbachs, 1982).

Two scenarios are often considered when evaluating assimilation of low- $\delta^{18}O$ crust: 1) assimilation of rhyolitic melts, resulting from remelting of altered and largely basaltic basic crust and 2) bulk or partial digestion (cannibalisation) of mafic low- $\delta^{18}O$ crust. For primitive basalts scenario 2 is often invoked to explain low- $\delta^{18}O$, as scenario 1 would result in a significant shift in major and trace element chemistry which has proved difficult to detect in Icelandic basalts (Breddam, 2002; Hartley et al., 2013).

A simple way of evaluating the effects from crustal assimilation on the dataset presented here involves considering possible

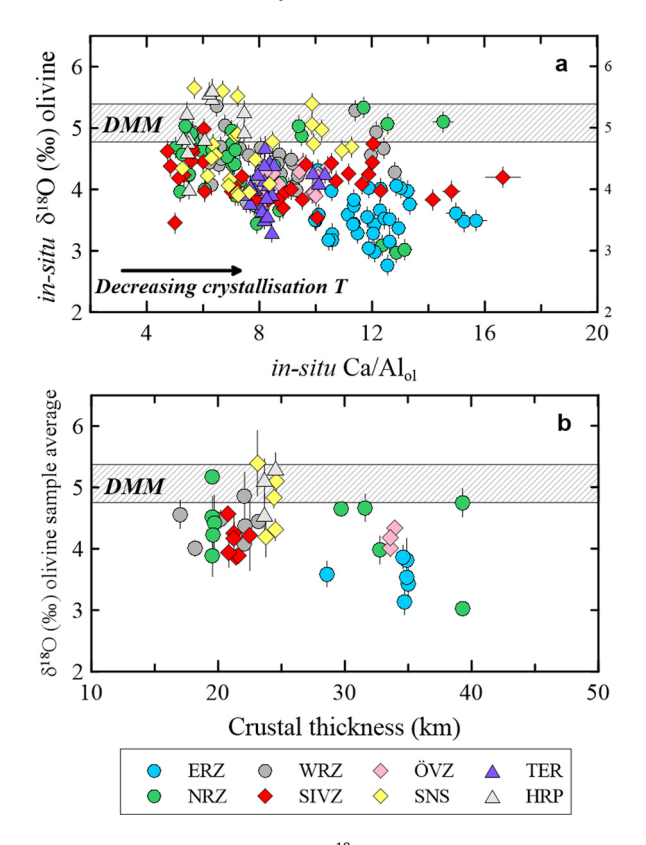


Fig. 4. Ca/Al_{ol} and crustal thickness with $\delta^{18}O_{ol}$. a) Higher Ca/Al_{ol} ratios, as representing lower crystallisation temperatures (Rasmussen et al., 2020), are associated with $\delta^{18}O_{ol}$ values below 4%, suggesting that values significantly below 4% are more likely to represent secondary crustal processes. A similar image is observed in b), where neovolcanic sample averaged $\delta^{18}O_{ol}$ values below 3.8% are all associated with crustal thicknesses exceeding 28 km (Jenkins et al., 2018). Olivine from locations with such thick crust are more likely to have been stored for a period of time in various magma reservoirs, increasing the likely effect from crustal assimilation. The crossed field represents the $\delta^{18}O$ of mantle-derived olivine from Eiler (2001). The errors associated with each data point correspond to the instrumental error (1SD).

correlations between $\delta^{18} O_{ol}$ and indicators of evolving melt compositions, such as olivine Fo values, Mn and Zn content, as crustal assimilation mostly follows melt evolution. However, except for a small group of olivine from NRZ, no overall correlation is evident between Fo values, Mn and Zn content and in-situ $\delta^{18} O_{ol}$ (Fig. 2), which differs from previous SIMS-based $\delta^{18} O_{ol}$ studies on large volume basalts from Iceland's Eastern Rift Zone (ERZ [Bindeman et al., 2008], see Fig. S5).

Integration of $\delta^{18}O_{ol}$ values with other proxies for crustal processes, such as the published same-spot Ca/Alol values (Rasmussen et al., 2020) - proposed to reflect relative olivine crystallisation temperatures (Gómez-Ulla et al., 2017) - could allow for a simple test of how susceptible the source melts were to possible crustal assimilation effects. Notably, olivine with Ca/Alol values <7 - recording the highest crystallisation temperatures - are mostly associated with $\delta^{18}O_{ol}$ values between 4.0-5.7% and Ca/Al_{ol} values >7 - reflecting lower crystallisation temperatures - are associated with $\delta^{18}O_{ol}$ values significantly below 4% (Fig. 4a). This observation applies to all olivine from ERZ and δ^{18} O values below 3.9% measured in NRZ, consistent with the NRZ olivine trend observed in Fig. 2. The apparent association between high Ca/AloI - representative of lower crystallisation temperatures – and $\delta^{18}O_{ol}$ below 4% can represent a scenario where the crystals with high Ca/Al values reside in magma channels, or reservoirs, longer and are thus more susceptible to inheriting δ^{18} O values that reflect assimilation of low- δ^{18} O crust. This hypothesis is supported by evidence suggesting that assimilation of hydrated crust in Iceland is a progressive process accompanying melt migration towards more shallow depths and fractional crystallisation, and largely occurs in the uppermost part of the crust (<7 km), where the heat released from crystallisation result in the assimilation of hydrated basalt (Caracciolo et al., 2022).

Thus, $\delta^{18}{\rm O}$ values in olivine with Ca/Al below 7, which represent olivine crystallised at higher temperatures, are more likely to be sourced from deeper in the crust and retain their initial $\delta^{18}{\rm O}$ melt values. Taking the effect from crystallisation temperatures into consideration, any $\delta^{18}{\rm O}_{\rm ol}$ values below 3.9% with Ca/Al_{ol} values >7 must be evaluated further before assigning a mantle source origin for their low $\delta^{18}{\rm O}$ characteristics.

5.1.2. Crustal thickness

The presence of a thick crust, as is common especially in central Iceland, permits extensive, trans-crustal magmatic plumbing systems that promote modification of mantle-derived melts via assimilation. Also, following isostatic subsidence, caldera collapses and burial within rifts, low- δ^{18} O material can be present at depths of up to 11 km and may interact with upwelling mantle-derived magmas (Hattori and Muehlenbachs, 1982). Therefore, assimilation of low δ^{18} O hydrated basaltic crust, leading to a lowering of mantlederived melt δ^{18} O values, can occur in the upper 11 km of the Icelandic crust (Hartley et al., 2013). Most of the Icelandic olivine crystals targeted here have high-forsterite values (Fo > Fo₈₅), suggesting crystallisation in the lower- to middle crust (>10 km, e.g., Neave and Putirka, 2017). These parts of the crust are likely dominated by intrusive materials characterised by canonical mantle-like δ^{18} O values (e.g., Hartley et al., 2013). As a result, any melt-crust interactions taking place there would therefore not lead to a lowering of the $\delta^{18}O_{melt}$ values.

Yet, basaltic melts from ERZ have been shown to be prone to assimilation processes as recorded in a number of moderate to largevolume tholeiitic basalts (e.g., Bindeman et al., 2008; Halldórsson et al., 2018). Indeed, barometry of melts from ERZ has highlighted the importance of shallow to mid-crustal (<8 km) magma reservoirs in this region where magmas stall, crystallise and homogenise prior to eruption (e.g., Caracciolo et al., 2020, Halldórsson et al., 2018). Incomplete shallow-storage homogenisation and diffusion processes may result in development of chemically zoned olivine with large ranges of δ^{18} O values (e.g., Bindeman et al., 2008), suggesting overprinting by low and crustally-inherited δ^{18} O values. Several moderate to large-volume basaltic lavas associated with the ERZ, including Laki and Holuhraun (Halldórsson et al., 2018; Bindeman et al., 2008), bear witness to mid- to lower-crustal assimilation processes, and thus highlight that some degree of filtering of olivine analyses must be carried out before assigning a source-derived $\delta^{18}O_{ol}$ value.

To test how varying crustal thicknesses may affect $\delta^{18}O_{ol}$ values, likely crustal thicknesses beneath each sample location were reconstructed using seismic data from Jenkins et al. (2018). At localities where the crustal thickness is around 20 km, the thinner crust for the samples studied here, the $\delta^{18}O_{ol}$ values vary between 3.9% in SIVZ (21 km) to 5.2% in NRZ (20 km), whereas $\delta^{18}O_{ol}$ values below 3.8% are all associated with crustal thicknesses above 28 km (Fig. 4b). A thicker crust could allow for the development of extensive plumbing systems, which in turn allows possible contamination from low- δ^{18} O_{ol} crust (altered at shallow levels), and thus will be important for evaluating possible effects of crustal assimilation in the dataset presented in this study. Rift dominated segments, which are often aligned with thick crust, could also represent regions with higher concentrations of fractures, caused by tectonic stress, allowing for deeper hydrothermal system penetration. However, abundant crustal fractures, and the presence of upper crustal magma storage in all the active volcanic regions in Iceland, makes tectonic controls difficult to estimate. Nonetheless, whether the effect from a thick crust is related to the plumbing system development or is affected by tectonic fractures, olivine with δ^{18} O values below 3.8% and thick crust will henceforward be evaluated with caution. Unlike the samples from the neovolcanic zones (see Fig. 1), the crustal thickness at eruption time for the TER samples is unknown (i.e., >1 Ma), and this method cannot be used to make a similar evaluation for these samples.

5.1.3. Characterising source-derived $\delta^{18}{\rm O}$ values in Icelandic high-forsterite olivine

A low- δ^{18} O component has previously been ascribed to geochemically-enriched and fusible mantle components, possibly representing recycled material residing in the Icelandic plume (Macpherson et al., 2005; Thirlwall et al., 2006; Winpenny and Maclennan, 2014; Shorttle and Maclennan, 2011). Extensive minorand trace-elemental variability, thought to reflect lithological heterogeneity carried by the Icelandic plume, is characteristic of the olivine crystals targeted here (Rasmussen et al., 2020). The sampling of this heterogeneity was argued to be controlled by various proportions of melt derived from olivine-rich peridotite and olivine-poor pyroxenite (Rasmussen et al., 2020), the latter resulting from incorporation of recycled oceanic crust. Minor and trace element ratios that are not expected to be changed by crustal processes, such as 100(Mn/Fe)ol and Mn/Znol (Mn/Fe and Mn/Zn hereafter), were found to be a particularly useful tracer of such lithological variability (Sobolev et al., 2007) and have previously been successfully applied to tracing the presence of pyroxenite in the Icelandic plume (Rasmussen et al., 2020).

To evaluate the δ^{18} O composition of this pyroxenitic component, δ^{18} O_{ol} values are plotted versus Mn/Fe and Mn/Zn (Fig. 3). Here, it becomes clear that most olivines with Mn/Fe < 1.5 – indicative of a more pyroxenitic source lithology (e.g., Sobolev et al., 2007; Rasmussen et al., 2020) – or olivine with lower Mn/Zn values have δ^{18} O_{ol} below DMM. In high-forsterite olivine, variable Mn/Fe and Mn/Zn traces mantle source(s) rather than crustal processes (Sobolev et al., 2007; Howarth and Harris, 2017), so any correlation between these ratios and δ^{18} O_{ol} must be source-controlled and cannot be an effect of crustal assimilation or other magmatic processes (Rasmussen et al., 2020). Variations in δ^{18} O_{ol} that are not manifested in Mn/Fe and Mn/Zn variability are therefore more likely to reflect crustal assimilation.

As discussed above, ERZ-derived magmas have been shown to be especially susceptible to assimilation processes and that their olivine crystals may not reflect primary, source-derived δ^{18} O. Indeed, ERZ olivines have near-uniform Mn/Fe values (between 1.57-1.64) but highly variable δ^{18} O values (between 2.77-4.32%). Olivines from the WRZ cluster around a $\delta^{18}O_{ol}$ value of 4.3% at Mn/Fe around 1.6, while NRZ olivines reveal highly heterogeneous δ^{18} O and Mn/Fe values (Fig. 3a). Thus, there is a large variation in $\delta^{18}O_{ol}$ at constant Mn/Fe, mostly towards $\delta^{18}O$ values below DMM which, following the arguments above, might be attributed crustal assimilation. However, olivine from WRZ with Fo values up to Fo₉₀₋₉₁ display δ^{18} O_{ol} values down to 3.8 \pm 0.2% at Mn/Fe of approximately 1.6 (Fig. 2a and 3a). Such high Fo values likely reflect crystallisation of olivine buffered by peridotite-olivine and were therefore crystallised within the mantle. Thus, this low $\delta^{18}O$ value from the WRZ reflects a robust lower limit for source-derived $\delta^{18}\mathrm{O}$ values identified here. Indeed, a previous SIMS-based study, targeting primitive plagioclase crystals from NRZ, identified mantlederived $\delta^{18}O_{ol}$ values down to 3.8% (Winpenny and Maclennan, 2014).

5.1.4. Isolating the mantle signature

To filter out samples that show potential signs of crustal assimilation in the dataset presented here, olivine that fulfil all the

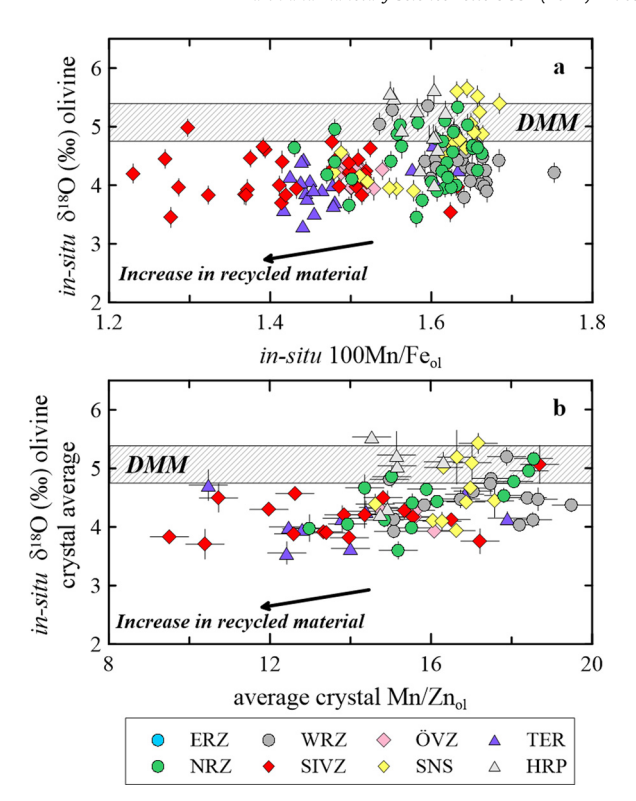


Fig. 5. Filtered $\delta^{18} O_{ol}$ values representing mantle-derived $\delta^{18} O_{ol}$ variation. To minimise $\delta^{18} O_{ol}$ values that may reflect crustal assimilation rather than source-derived $\delta^{18} O$ values, observations from crustal process proxies presented in section 5.1.1-5.1.3 were combined and any olivine datapoint that fulfil these three criterias: (i) have Ca/Al > 7, (ii) come from thick crust localities (>28 km), and (iii) have near-constant 100 Mn/Fe values ~ 1.6 were excluded from further evaluation of source-derived $\delta^{18} O$ values (see text for details). The filtering of the data highlights a positive trend between tracers of source lithology and $\delta^{18} O_{ol}$ values with $r^2 = 0.138$ and a p-value of $\ll 0.01$ (for Mn/Fe) and r^2 of 0.157 and a p-value of $\ll 0.01$ (for Mn/Zn). The crossed field represents the $\delta^{18} O$ of mantle-derived olivine from Eiler (2001). The errors associated with each data point correspond to the instrumental error (1SD).

following criteria: (i) have Ca/Al > 7, (ii) come from thick crust localities (>28 km), and (iii) have near-constant Mn/Fe values between 1.57-1.64 and $\delta^{18}O_{ol}$ below 3.8% are excluded from further evaluation of source-derived δ^{18} O values. Moreover, due to the abundant evidence of crustal assimilation playing an important role in the ERZ, all $\delta^{18}O_{ol}$ values below that of DMM are excluded as a precaution. Filtering the data according to the three conditions presented here, $\delta^{18}O_{ol}$ values down to 3.5% remain, indicating that a low δ^{18} O component is a likely feature of the Iceland mantle (Fig. 5). Statistical evaluation of the filtered dataset confirms the observation where a reduction of $\delta^{18}O_{ol}$ is overall associated with lower Mn/Fe ($r^2 = 0.138$; p-value of $\ll 0.01$ suggesting statistical significance) and Mn/Zn ($r^2 = 0.157$; p-value of \ll 0.01 [Fig. 5]). Considering this approach, a low- δ^{18} O (down to \sim 3.5% in SIVZ) can be associated with a greater contribution from pyroxenite-derived (and thereby recycled crust-derived) melting in the sub-Iceland mantle, akin to findings from other ocean islands (e.g., Day and Hilton, 2011). Examples of filtering using the individual criteria separately are presented in supplement 1.5.

Previous findings support the conclusion of a low- $\delta^{18}O$ component associated with enriched components within the Iceland mantle (e.g., Macpherson et al., 2005; Winpenny and Maclennan, 2014), and a similarly low- $\delta^{18}O$ source component was even recognised in submarine basalts from Reykjanes Ridge that cannot have interacted with low $\delta^{18}O$ meteoric water (Thirlwall et al., 2006). Finally, bulk assimilation of hyaloclastites is unlikely to account for low $\delta^{18}O_{ol}$ observed in older formations outside the neovolcanic

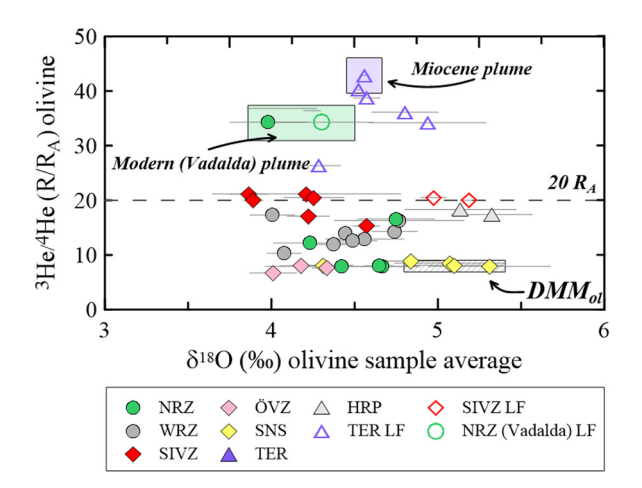


Fig. 6. 3 He/ 4 He $_{ol}$ vs. δ^{18} O $_{ol}$ values for the same samples. All crystals with 3 He/ 4 He $_{ol}$ values $\gg 20$ R $_{A}$ display δ^{18} O $_{ol}$ values below $5.1 \pm 0.3\%$ (DMM) whereas samples with 3 He/ 4 He $_{ol}$ values < 20R $_{A}$ display a large variation between 4% and 5.4%. The SIMS data are represented by filled symbols while the LF data are represented by unfilled symbols.

zones (TER and HRP) as hyaloclastites were not present in significant amounts before 3 Ma (Carley et al., 2020), suggesting that the presence of a low δ^{18} O component in the Icelandic mantle has been a feature of the plume for at least the last 15 Ma.

5.2. A low- δ^{18} O Iceland plume: constraints from 3 He/ 4 He

The samples studied here have previously been characterised for ${}^{3}\text{He}/{}^{4}\text{He}$ (Harðardóttir et al., 2018; Jackson et al., 2020). Focusing exclusively on samples that have not experienced posteruptive radiogenic ${}^{4}\text{He}$ ingrowth (see supplement 1.6) ${}^{3}\text{He}/{}^{4}\text{He} > 8R_A$ (i.e., values higher than DMM) provides unambiguous evidence for primordial components carried within the Icelandic plume (Harðardóttir et al., 2018), and allows for an evaluation of the extent to which the upwelling plume component controls the distribution of low- $\delta^{18}\text{O}$ in the Icelandic mantle (Fig. 6).

Icelandic olivine crystals with ${}^3\text{He}/{}^4\text{He} \gg 20\text{R}_A$, or ratios significantly above DMM, have $\delta^{18}\text{O}_{ol} < 5.1 \pm 0.3\%$ (i.e., below the range characteristic for DMM), whereas olivine with ${}^3\text{He}/{}^4\text{He} \ll 21\text{R}_A$ (e.g., WRZ, NRZ, SNS and HRP) reveal a larger range in $\delta^{18}\text{O}_{ol}$ (4.0-5.4%, Fig. 6) that partly overlaps with DMM. The higher ${}^3\text{He}/{}^4\text{He}$ values represent sampling of pristine plume-related melts and $\delta^{18}\text{O}_{ol}$ for the TER sample with the highest ${}^3\text{He}/{}^4\text{He}$ of 42.9R_A (Fig. 6) is $4.6 \pm 0.1\%$ (1SD). Based on these observations, this set of values best represent the pristine ${}^3\text{He}/{}^4\text{He} - \delta^{18}\text{O}$ composition of the *Miocene* plume. Olivine from the Vaðalda shield volcano carries the highest ${}^3\text{He}/{}^4\text{He}$ in the neovolcanic zone (34.3R_A) and has corresponding $\delta^{18}\text{O}_{ol}$ of $4.2 \pm 0.3\%$, which is slightly lower than the *Miocene* plume. Based on the presence of the highest ${}^3\text{He}/{}^4\text{He}_{ol}$ values in Vaðalda and in line with prior studies (Hilton et al., 2000; Jackson et al., 2020), the He-O isotopic characteristic of Vaðalda therefore best represent the *Modern* plume component.

5.3. Entrainment of oceanic lithosphere into the Iceland plume

The 60 Ma Baffin Island picrites associated with onset of hotspot volcanism above the *Proto*-Iceland plume are characterised by the highest ${}^{3}\text{He}/{}^{4}\text{He}$ measured in any ocean island (up to $50R_{A}$, Starkey et al., 2009) and likely sourced from a reservoir with ${}^{3}\text{He}/{}^{4}\text{He}$ values up to $60R_{A}$ (Mundl-Petermeier et al., 2019). Apart from ${}^{3}\text{He}/{}^{4}\text{He}$, Baffin lavas are characterised by DMM-like isotopic compositions and average $\delta^{18}O_{ol}$ of 5.1% (5.03-5.21%, Willhite et al., 2019). When comparing the *Proto*, *Miocene* and *Modern* Iceland plume, a coupled lowering of $\delta^{18}O_{ol}$ (from 5.1 to 4.2%) and

 3 He/ 4 He $_{\rm ol}$ (from 60 to 34R_A) is therefore evident suggesting that a component with lower δ^{18} O and 3 He/ 4 He has been introduced over time.

A likely candidate for this low $\delta^{18}O$ and low ${}^{3}He/{}^{4}He$ component present in the Iceland plume after 60 Ma is recycled oceanic lithosphere (ROL, Day and Hilton, 2011; Macpherson et al., 2005). Indeed, incorporation of ROL has frequently been proposed to explain the geochemical shift to higher ⁸⁷Sr/⁸⁶Sr, ²⁰⁶Pb/²⁰⁴Pb and ¹⁸⁷Os/¹⁸⁸Os for the *Modern* versus the *Proto* plume component (Kokfelt et al., 2006; Hartley et al., 2013; Dale et al., 2009; Brandon et al., 2007) and can explain the presence of secondary pyroxenite in the Iceland plume as shown by trace element variations in olivine (Rasmussen et al., 2020). Here, ROL is characterised by δ^{18} O down to $\sim 2\%$, based on previous suggestions and type II eclogite compositions that likely represent recycled oceanic lithosphere unaffected by later metasomatic events (Macpherson et al., 2005; Gréau et al., 2011) and ${}^{3}\text{He}/{}^{4}\text{He}$ between 0.01-6R_A, where the exact ³He/⁴He values and He concentrations depend on the age of ROL (data supplement T6, Brandon et al., 2007). Because the concentration of O is essentially identical in the various mantle components, this variable is irrelevant for the mixing models presented below.

The Miocene and Modern Iceland plume compositions can be replicated by use of a simple two-component mixing model between a 1 Ga basalt (representing ROL, Brandon et al., 2007), with $\delta^{18}\text{O}$ of 2\% and ${}^{3}\text{He}/{}^{4}\text{He}$ of 2.3R_A, and a *Proto* plume source with δ^{18} O of 5.1% and 3 He/ 4 He of 60R_A (orange line, Fig. 7a). Here, the various hybrid plume compositions (Miocene, green box, and Modern plume, purple box, each corresponding to a certain mixture of the Proto plume and ROL) are best simulated when the Proto plume is assumed to have \sim 22 times the ³He content of DMM (DMM = $4.4 \cdot 10^{-11} \text{cc}^3 \text{He/g}$, Porcelli and Ballentine, 2002; i.e., ${}^{3}\text{He}_{\text{proto plume}}/{}^{3}\text{He}_{\text{DMM}} \sim 22$, data supplement T6). When constructing this mixing model, the focus is on relative ³He enrichments in the plume source relative to DMM rather than ⁴He, following the approach described in Hilton et al. (2000). This mixing model shows that the *Miocene* plume can be replicated when 18% ROL is incorporated into a Proto plume while 30% ROL is necessary to replicate the Modern plume (Fig. 7a). The temporal increase in the influence of recycled material on the composition of the Iceland plume is supported by data from Pb isotopes where the most radiogenic samples over this history of the Iceland hotspot are found in recent volcanics from SIVZ which also represent the region with the strongest signal from ROL as traced by minor and trace elements (Fig. 5).

The model results in ³He_{plume}/³He_{DMM} enrichment for the Miocene and Modern plume of 18 and 16, respectively, which corresponds well with values proposed by Gonnermann and Mukhopadhyay (2007) for global plume sources and values proposed by Hilton et al. (2000) for the Iceland plume source, supporting our initial assumptions for the ³He content of the proto plume. The chosen age of the recycled component used for this model (1 Ga) is based on lower estimated model ages from Os and Pb isotopes (Brandon et al., 2007; Kokfelt et al., 2006). However, other estimates suggest a much younger Phanerozoic age for the recycled component in the Iceland plume (e.g., Thirlwall et al., 2004; Halldórsson et al., 2016). Yet, it must be highlighted that changing the age of the recycled crust between 1 Ga and 250 Ma results in insignificant variations in the relative ROL amounts (by 1% for the Miocene and 2% for the Modern plume). However, this change requires that the ${}^{3}\text{He}_{\text{proto plume}}/{}^{3}\text{He}_{\text{DMM}}$ enrichment – representing the enrichment of ³He in the *Proto plume* relative to DMM – is adjusted to \sim 5 (for 250 Ma ROL) or to \sim 11 (for 500 Ma ROL) in order for the mixing lines (orange, green and purple lines in Fig. 7) to describe the data. Note that these values are all still within previ-

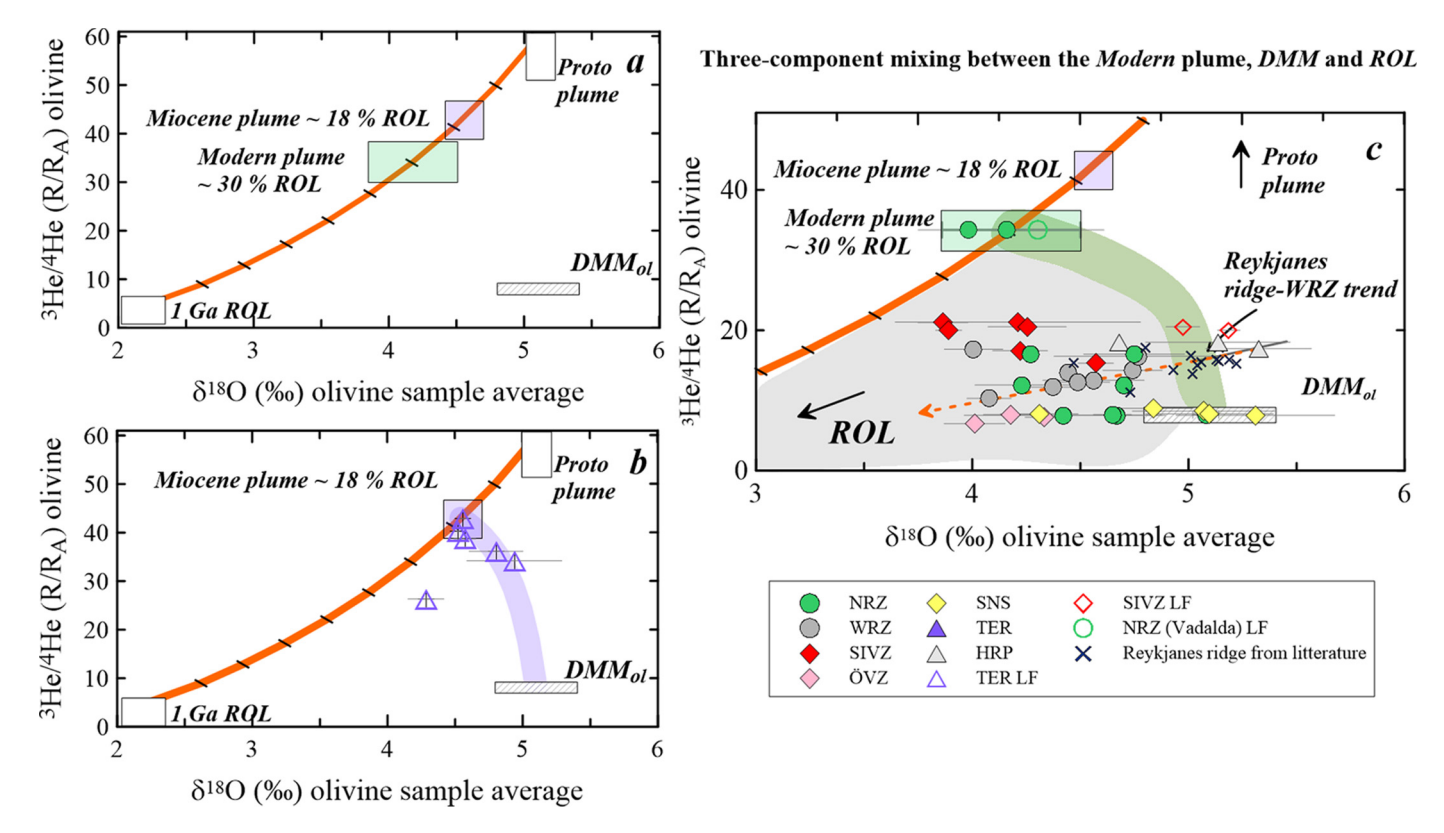


Fig. 7. δ^{18} O (SIMS and LF)- 3 He/ 4 He systematics of Icelandic olivine. a) Mixing between the Proto Iceland plume (δ^{18} O = 5.1% 3 He/ 4 He = 60 R_A) and a 1 Ga recycled oceanic lithosphere (ROL, δ^{18} O $\sim 2\%$, 3 He/ 4 He = 0.01-6R_A, orange line) can replicate the Miocene (δ^{18} O = 4.6 \pm 0.1% 3 He/ 4 He = 42.9R_A) and Modern (δ^{18} O = 4.2 \pm 0.3%, 3 He/ 4 He = 34.3R_A) plume components - reflecting the highest 3 He/ 4 He sampled by Tertiary and neovolcanic Iceland olivine - when the Proto plume component has 3 He concentrations 22 times those of DMM. This mixing results in 3 He_{plume}/ 3 He_{DMM} enrichment to decrease to 18 for the Miocene plume and 16 for the Modern plume which in turn controls the curves for mixing between these hybrid plume compositions and DMM (see Hilton et al., 2000). To explain the pattern presented by the Tertiary (b), Plio-Pleistocene and neovolcanic (c) dataset, DMM must be invoked (δ^{18} O_{ol} = 4.8-5.4% 3 He/ 4 He 7-9R_A), which is also reflected in SNS olivine and data from NRZ from Macpherson et al. (2005). Mixing between the Miocene (b, purple line) or the Modern plume (c, green line) and DMM creates an umbrella of compositions that can further mix with ROL in the upper mantle, representing the result of three-component mixing (example by light grey field in 7c). An example of this is seen in the data from WRZ, HRP and previously published data from Reykjanes ridge (c, Thirlwall et al., 2006; Hilton et al., 2000) where a Modern plume:DMM mixture of 15:85 creates an endmember for further mixing with ROL (highlighted by the orange arrow). The exact composition of the various endmembers used for the mixing is available in the data supplement T6. The SIMS data are represented by filled symbols while the LF data are represented by unfilled symbols. The crosses represent literature LF data from Reykjanes Ridge from Thirlwall et al., 2006; Eiler et al., 2000). The square size for ROL is for illustra

ous estimates (e.g., Hilton et al., 2000) and thus, this consideration makes little difference for this study.

5.4. The role of DMM in the Iceland mantle

Mixing between a hybrid Iceland plume and a *DMM* component has previously been shown to explain variations in He-N-Pb isotopic systematics of Icelandic and Reykjanes Ridge basalts (Halldórsson et al., 2016; Hilton et al., 2000). Additionally, He-O isotope values akin to *DMM* are directly recorded in the dataset by olivine from SNS (Fig. 7c) – a region previously suggested to lack plume-derived melt inputs altogether (Rasmussen et al., 2020) – supporting its role in the Iceland mantle.

Indeed, introducing *DMM* to the mixture of components in the Icelandic mantle provides a simple means to describe the spread of data observed in Fig. 7c. Based on the result from the mixing model presented in section 5.3, the ³He_{plume}/³He_{DMM}, which controls the shape of the mixing curve (Hilton et al., 2000), has decreased to 18 for the *Miocene* plume and 16 for the *Modern* plume, which allows for modelling of the mixing curve between the hybrid plume components and DMM shown in Fig. 7b (purple line) and 7c (green line). This mixing line between the *hybrid* plume and *DMM* (purple line, Fig. 7b, green line, Fig. 7c) represents an endmember 'umbrella' for further mixing with *ROL* carried within the Icelandic plume. An indication of this process is visible in data from HRP, WRZ, and published data from Reykjanes ridge

(Fig. 7c, Hilton et al., 2000; Thirlwall et al., 2006). Here, olivine from Reykjanes ridge is described by a Modern plume:DMM mixture of approximately 15:85. The WRZ-Reykjanes ridge data trend (Fig. 7c, highlighted by an orange dashed arrow) can thus be explained by mixing between this Reykjanes ridge endmember and ROL. Evidence of mixing between components plotting along the Modern plume-DMM mixing line (green line, Fig. 7c) and ROL suggests that the incorporation of ROL occurs in the upper mantle too, perhaps following delamination of altered lithosphere. Consequently, incorporation of ROL likely occurs both deeply in the plume, as reflected by pure and thorough Proto plume-ROL mixing (retaining high ³He/⁴He values with no evidence for DMM presence), and at more shallow mantle depths where DMM is introduced, as reflected by contemporary three-component mixing between the Modern plume, DMM and ROL. The exact presence of ROL in the upper mantle cannot be determined based on the new data presented here. However, for the purpose of this study this parameter is unimportant and will not be discussed further.

Thus, it can be concluded that the He and O isotopic evolution of the Iceland plume can be replicated by mixing between three main mantle endmembers: *Proto* plume, *DMM* and *ROL*. Moreover, the He-O patterns presented in Fig. 7c are consistent with previous findings supporting the hypothesis that central (Vaðalda) and south Iceland (SIVZ) represents regions with the highest degree of plume-fed melts, characterised by low δ^{18} O and high 3 He/ 4 He val-

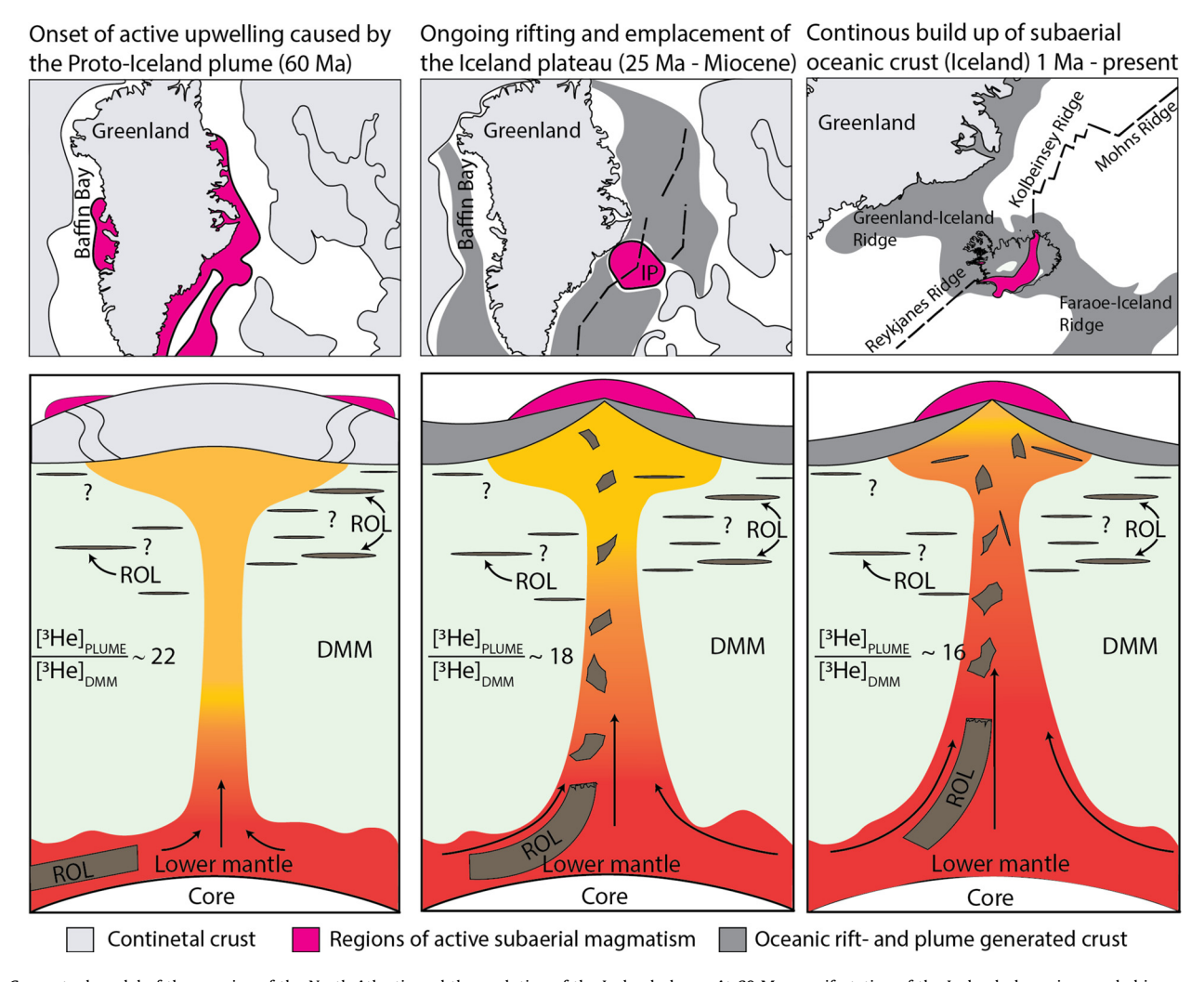


Fig. 8. Conceptual model of the opening of the North Atlantic and the evolution of the Iceland plume. At 60 Ma, manifestation of the Iceland plume is recorded in magmatism along the borders of Greenland. At this time, the Proto plume is enriched in ³He relative to DMM (³He_{PLUME})³He_{DMM}) by a factor of 22. Enhanced melt production leading to the formation of the Iceland Plateau (IP) at 25 Ma coincides with an increase in plume temperature, plume flux and the appearance of recycled oceanic lithosphere (ROL) as traced by He-O isotopic systematics. The appearance of ROL along with an increase in plume flux suggests, that the increased plume flux led to enhanced entrainment of dense high ³He/⁴He domains and ROL stored at depth and possibly as delaminated altered lithosphere in the upper mantle. Moreover, tectonic changes in the North Atlantic between 30-25 Ma led to the alignment between the Iceland plume head and the ongoing North Atlantic rift, which likely promoted enhanced melting in the Iceland plume. Thus, the formation of the IP around 25 Ma is a result of temporal changes in the Iceland plume and plate reorganisation of the North Atlantic. Today, the plume-related magmatism (in pink) is centred beneath Iceland which has further promoted plume-related melting. The incorporation of ROL, and thereby addition of ⁴He to the Iceland plume, over time is reflected in a lowering of the ³He_{PLUME}/³He_{DMM} from 22 in the Proto plume to 16 in the Modern plume.

ues, while melts from NRZ and WRZ reveal an affinity towards more DMM-like δ^{18} O and 3 He/ 4 He values, and SNS shows a lack of plume contribution altogether (Rasmussen et al., 2020).

5.5. Implications for temporal variations in activity of the Iceland plume

Initiation and manifestation of the Iceland plume occurred at ${\sim}60$ Ma, which led to continental break-up (at ${\sim}55$ Ma) and initiation of North Atlantic basin formation (Fig. 8, Holbrook et al., 2001). In the Late Eocene (${\sim}35$ Ma) plume activity rapidly decreased, causing relative thinning of the oceanic lithosphere and ocean floor subsidence (Holbrook et al., 2001; Abelson et al., 2008; Parnell-Turner et al., 2014). Plume activity increased again ${\sim}25$ Ma as evident from enhanced magma production related to the formation of the Iceland Plateau (Fig. 8, Holbrook et al., 2001; Abelson et al., 2008). The Iceland Plateau (IP) has long been a puzzling topographic feature in the North Atlantic with its near-circular outline and propagating V-shaped ridges extending to the South (Fig. 1, Ito, 2001). This study proposes the hypothesis that the increase in plume activity, which lead to the formation of the IP, was a result of an increase in plume temperature, plume buoyancy and flux –

which likely led to enhanced entrainment of recycled lithosphere – and the contemporary alignment of the North Atlantic Ridge and the Iceland plume head around the same time.

High ³He/⁴He plumes, such as the Iceland plume, are associated with hotter mantle temperatures (Jackson et al., 2017), suggesting that primordial high-³He/⁴He domain must be deep and dense such that only the most buoyant plumes - which must be the hottest - entrain it. Previous studies have concluded that the temperature of the Iceland plume increased following a temperature low around 35 Ma (Spice et al., 2016). As a result, this temperature increase must be accompanied by an increase in plume buoyancy and/or plume flux, thereby making the plume capable of entraining dense high ³He/⁴He domains. While the *Proto*-Iceland plume shows no evidence of ROL, the formation of the IP - resulting from enhanced plume-related melt production as described above - coincides with the appearance of ROL in the Iceland plume. The increase in plume flux and the contemporary appearance of ROL suggests that the increase in plume activity at \sim 25 Ma - as associated with enhanced entrainment of previously deeply stored, dense high ³He/⁴He domains – must be related to the entrainment of ROL (Fig. 8). This dense lower mantle reservoir is likely characterised by high ${}^3\text{He}/{}^4\text{He}$ and DMM-like $\delta^{18}\text{O}$, a commonly observed trait of other high- ${}^3\text{He}/{}^4\text{He}$ mantle plumes (Day and Hilton, 2011; Starkey et al., 2016), while concurrent incorporation of ${}^4\text{He}$ -rich *ROL* serves to counter the increase in ${}^3\text{He}/{}^4\text{He}_{\text{plume}}$ otherwise expected from enhanced entrainment of dense lower mantle material. Coupled lowering of $\delta^{18}\text{O}$ and ${}^3\text{He}/{}^4\text{He}$ in the *Miocene* and *Modern* plume, relative to the *Proto*-Iceland plume, can therefore effectively be attributed the degree of incorporation of *ROL* somewhere in the plume stem as has also been observed for other hot spots such as the Canary Islands and Hawaii (Day and Hilton, 2011; Lassiter and Hauri, 1998).

Alignment of the North Atlantic rift and the Iceland plume head occurred between 30-25 Ma (Howell et al., 2014), around the same time of the formation of the IP. The coincidence of these two events suggests that the tectonic change, from a setting where the Iceland plume was overlain by thick continental crust to thin oceanic crust, assisted and promoted melting in the Iceland plume. Upon emplacement of the IP, plume activity became concentrated beneath the active rift systems (Fig. 8) which further promoted melting by additional tectonic-aided upwelling. As was the case for the Proto-Iceland plume, many large igneous provinces erupt through a thick continental crust, which results in chemical fingerprints reflecting both mantle and continental crust signatures (Willhite et al., 2019; Carlson et al., 1981). Because of plate reorganisation in the North Atlantic, the Iceland hot spot activity transitioned to an oceanic setting by 30-25 Ma (Howell et al., 2014), facilitating identification of changes driven by mantlederived upwellings. Thus, the Iceland Plateau represents a unique surficial expression recording a temporally evolving mantle plume source. This temporal evolution is reflected in $\delta^{18}O_{ol}$ - $^{3}He/^{4}He_{ol}$ space which highlights the usefulness of combining these systems when evaluating chemical traits of an evolving plume.

6. Conclusion

This study is the first large-scale study that obtains both high-quality in-situ and bulk crystal δ^{18} O measurements from a large sample set of primitive olivine crystals to investigate controls on low- δ^{18} O values characteristic of Icelandic basalt. Through careful consideration of various crustal processes which may modify primary δ^{18} O₀l values, this study found that:

- 1. Low $\delta^{18} O_{ol}$ values, down to 3.5% are present in the Iceland mantle.
- 2. When combined with published 3 He/ 4 He_{ol} values for the same samples, low- δ^{18} O values likely reflect incorporation of recycled oceanic lithosphere (*ROL*) into the Iceland plume.
- 3. The amount of *ROL* incorporated into the Iceland plume has increased since the initiation of the plume 60 Ma to 18% in the Miocene and 30% today. This increase likely results from enhanced melting within the Iceland plume following the alignment of the plume head and the North Atlantic rift around the formation time of the Iceland plateau \sim 25 Ma.
- 4. The findings presented in this article reflect a unique case highlighting a temporally evolving mantle plume.

CRediT authorship contribution statement

MBR has been responsible for sample prep and measurements by SIMS in Sweden and EMPA work in Iceland under the guidance of SAH and MJW. MGJ provided the TER samples analysed by LF and these analyses, along with LF analyses of neovolcanic samples, were done by INB. Everyone has been involved in the finalisation of this manuscript.

Declaration of competing interest

The authors declare that they have no known competing financial interests or personal relationships that could have appeared to influence the work reported in this paper.

Acknowledgements

The authors would like to thank Barbara Kleine for help with retrieving the SIMS data and Guðmundur Guðfinnsson, Lori Willhite, Rebekka Rúnarsdóttir and Kerstin Lindén for assistance with microprobe analysis and sample prep. A special thank you to Sunna Harðardóttir for providing crustal thicknesses and Jaime Barnes and Edward Marshall for providing the San Carlos standard. Thanks to Eemu Ranta, Edward Marshall, Sally Gibson, Simon Matthews, Thomas Kokfelt and Paul Martin Holm for helpful discussions and Bryndís Brandsdóttir for help with the acquisition of a map for Fig. 1. We furthermore thank Dr. Rajdeep Dasgupta for the handling of this publication and three anonymous reviewers for their expertise review which greatly improved the manuscript.

This work was funded by the Nordic Volcanological Center. MBR and SAH further acknowledges support from the Icelandic Research Fund (Grant #196084-051 and #196139-051). INB acknowledges support from NSF EAR 1822977. The NordSIMS facility acknowledges funding by the Swedish Research Council (infrastructure grant 2017-00671); this is NordSIMS publication #714. MGJ acknowledges NSF grant EAR-1900652.

Appendix A. Supplementary material

Supplementary material related to this article can be found online at https://doi.org/10.1016/j.epsl.2022.117691.

References

- Abelson, M., Agnon, A., Almogi-Labin, A., 2008. Indications for control of the Iceland plume on the Eocene–Oligocene "greenhouse-icehouse" climate transition. Earth Planet. Sci. Lett. 265 (1–2), 33–48.
- Bindeman, I., Gurenko, A., Carley, T., Miller, C., Martin, E., Sigmarsson, O., 2012. Silicic magma petrogenesis in Iceland by remelting of hydrothermally altered crust based on oxygen isotope diversity and disequilibria between zircon and magma with implications for MORB. Terra Nova 24 (3), 227–232. https://doi.org/10.1111/j.1365-3121.2012.01058.x.
- Bindeman, I., Gurenko, A., Sigmarsson, O., Chaussidon, M., 2008. Oxygen isotope heterogeneity and disequilibria of olivine crystals in large volume Holocene basalts from Iceland: evidence for magmatic digestion and erosion of Pleistocene hyaloclastites. Geochim. Cosmochim. Acta 72 (17), 4397–4420. https:// doi.org/10.1016/j.gca.2008.06.010.
- Brandon, A.D., Graham, D.W., Waight, T., Gautason, B., 2007. ¹⁸⁶Os and ¹⁸⁷Os enrichments and high-³He/⁴He sources in the Earth's mantle: evidence from Icelandic picrites. Geochim. Cosmochim. Acta 71 (18), 4570–4591.
- Breddam, K., 2002. Kistufell: primitive melt from the Iceland mantle plume. J. Petrol. 43 (2), 345–373.
- Caracciolo, A., Halldórsson, S.A., Bali, E., Marshall, E.W., Jeon, H., Whitehouse, M.J., Barnes, J.D., Guðfinnsson, G.H., Kahl, M., Hartley, M.E., 2022. Oxygen isotope evidence for progressively assimilating trans-crustal magma plumbing systems in Iceland. Geology. https://doi.org/10.1130/G49874.1.
- Caracciolo, A., Bali, E., Guðfinnsson, G.H., Kahl, M., Halldórsson, S.A., Hartley, M.E., Gunnarsson, H., 2020. Temporal evolution of magma and crystal mush storage conditions in the Bárðarbunga-Veiðivötn volcanic system, Iceland. Lithos 352–353, 105234. https://doi.org/10.1016/j.lithos.2019.105234.
- Carley, T.L., Miller, C.F., Fisher, C.M., Hanchar, J.M., Vervoort, J.D., Schmitt, A.K., Economos, R.C., Jordan, B.T., Padilla, A.J., Banik, T.J., 2020. Petrogenesis of silicic magmas in Iceland through space and time: the isotopic record preserved in zircon and whole rocks. J. Geol. 128 (1), 1–28. https://doi.org/10.1086/706261.
- Carlson, R.W., Lugmair, G.W., Macdougall, J.D., 1981. Crustal influence in the generation of continental flood basalts. Nature 289 (5794), 160–162. https://doi.org/10.1038/289160a0.
- Dale, C., Pearson, D., Starkey, N., Stuart, F., Ellam, R., Larsen, L., Fitton, J., Macpherson, C., 2009. Osmium isotopes in Baffin Island and West Greenland picrites: Implications for the ¹⁸⁷Os/¹⁸⁸Os composition of the convecting mantle and the nature of high ³He/⁴He mantle. Earth Planet. Sci. Lett. 278 (3–4), 267–277.

- Day, J.M., Hilton, D.R., 2011. Origin of ³He/⁴He ratios in HIMU-type basalts constrained from Canary Island lavas. Earth Planet. Sci. Lett. 305 (1–2), 226–234.
- Eiler, J., 2001. Oxygen isotope variations of basaltic lavas and upper mantle rocks. Rev. Mineral. Geochem. 43.
- Eiler, J., Grönvold, K., Kitchen, N., 2000. Oxygen isotope evidence for the origin of chemical variations in lavas from Theistareykir volcano in Iceland's northern volcanic zone. Earth Planet. Sci. Lett. 184 (1), 269–286.
- Eiler, J.M., Farley, K.A., Valley, J.W., Stolper, E.M., Hauri, E.H., Craig, H., 1995. Oxygen isotope evidence against bulk recycled sediment in the mantle sources of Pitcairn Island lavas. Nature 377 (6545), 138–141.
- Gautason, B., Muehlenbachs, K., 1998. Oxygen isotopic fluxes associated with hightemperature processes in the rift zones of Iceland. Chem. Geol. 145 (3–4), 275–286
- Gonnermann, H.M., Mukhopadhyay, S., 2007. Non-equilibrium degassing and a primordial source for helium in ocean-island volcanism. Nature 449 (7165), 1037.
- Gómez-Ulla, A., Sigmarsson, O., Gudfinnsson, G.H., 2017. Trace element systematics of olivine from historical eruptions of Lanzarote, Canary Islands: constraints on mantle source and melting mode. Chem. Geol. 449, 99–111.
- Gréau, Y., Huang, J.-X., Griffin, W.L., Renac, C., Alard, O., O'Reilly, S.Y., 2011. Type I eclogites from Roberts Victor kimberlites: products of extensive mantle metasomatism. Geochim. Cosmochim. Acta 75 (22), 6927–6954. https://doi.org/10.1016/j.gca.2011.08.035.
- Halldórsson, S.A., Bali, E., Hartley, M.E., Neave, D.A., Peate, D.W., Guðfinnsson, G.H., Bindeman, I., Whitehouse, M.J., Riishuus, M.S., Pedersen, G.B.M., Jakobsson, S., Askew, R., Gallagher, C.R., Guðmundsdóttir, E.R., Gudnason, J., Moreland, W.M., Óskarsson, B.V., Nikkola, P., Reynolds, H.I., Schmith, J., Thordarson, T., 2018. Petrology and geochemistry of the 2014–2015 Holuhraun eruption, central Iceland: compositional and mineralogical characteristics, temporal variability and magma storage. Contrib. Mineral. Petrol. 173 (8), 64. https://doi.org/10.1007/s00410-018-1487-9.
- Halldórsson, S.A., Hilton, D.R., Barry, P.H., Füri, E., Grönvold, K., 2016. Recycling of crustal material by the Iceland mantle plume: new evidence from nitrogen elemental and isotope systematics of subglacial basalts. Geochim. Cosmochim. Acta 176, 206–226.
- Harðardóttir, S., Halldórsson, S.A., Hilton, D.R., 2018. Spatial distribution of helium isotopes in Icelandic geothermal fluids and volcanic materials with implications for location, upwelling and evolution of the Icelandic mantle plume. Chem. Geol. https://doi.org/10.1016/j.chemgeo.2017.05.012.
- Hartley, M.E., Thordarson, T., Fitton, J.G., Eimf, 2013. Oxygen isotopes in melt inclusions and glasses from the Askja volcanic system, North Iceland. Geochim. Cosmochim. Acta 123, 55–73. https://doi.org/10.1016/j.gca.2013.09.008.
- Hattori, K., Muehlenbachs, K., 1982. Oxygen isotope ratios of the Icelandic crust. J. Geophys. Res., Solid Earth 87 (B8), 6559–6565. https://doi.org/10.1029/ JB087iB08p06559.
- Hilton, D.R., Thirlwall, M.F., Taylor, R.N., Murton, B.J., Nichols, A., 2000. Controls on magmatic degassing along the Reykjanes Ridge with implications for the helium paradox. Earth Planet. Sci. Lett. 183 (1–2), 43–50.
- Holbrook, W.S., Larsen, H., Korenaga, J., Dahl-Jensen, T., Reid, I.D., Kelemen, P., Hopper, J., Kent, G., Lizarralde, D., Bernstein, S., 2001. Mantle thermal structure and active upwelling during continental breakup in the North Atlantic. Earth Planet. Sci. Lett. 190 (3–4), 251–266.
- Howarth, G.H., Harris, C., 2017. Discriminating between pyroxenite and peridotite sources for continental flood basalts (CFB) in southern Africa using olivine chemistry. Earth Planet. Sci. Lett. 475, 143–151.
- Howell, S.M., Ito, G., Breivik, A.J., Rai, A., Mjelde, R., Hanan, B., Sayit, K., Vogt, P., 2014. The origin of the asymmetry in the Iceland hotspot along the Mid-Atlantic Ridge from continental breakup to present-day. Earth Planet. Sci. Lett. 392, 143–153. https://doi.org/10.1016/j.epsl.2014.02.020.
- Isa, J., Kohl, I., Liu, M.-C., Wasson, J., Young, E., McKeegan, K., 2017. Quantification of oxygen isotope SIMS matrix effects in olivine samples: correlation with sputter rate. Chem. Geol. 458, 14–21.
- Ito, G., 2001. Reykjanes 'V'-shaped ridges originating from a pulsing and dehydrating mantle plume. Nature 411 (6838), 681–684.
- Jackson, M.G., Blichert-Toft, J., Halldórsson, S.A., Mundl-Petermeier, A., Bizimis, M., Kurz, M.D., Price, A.A., Harðardóttir, S., Willhite, L.N., Breddam, K., Becker, T.W., Fischer, R.A., 2020. Ancient helium and tungsten isotopic signatures preserved in mantle domains least modified by crustal recycling. Proc. Natl. Acad. Sci., 202009663. https://doi.org/10.1073/pnas.2009663117.
- Jackson, M.G., Konter, J.G., Becker, T.W., 2017. Primordial helium entrained by the hottest mantle plumes. Nature 542 (7641), 340–343. https://doi.org/10.1038/ nature/21023
- Jenkins, J., Maclennan, J., Green, R.G., Cottaar, S., Deuss, A.F., White, R.S., 2018. Crustal formation on a spreading ridge above a mantle plume: receiver function imaging of the Icelandic crust. J. Geophys. Res., Solid Earth 123, 5190–5208. https://doi.org/10.1029/2017JB015121.

- Kokfelt, T.F., Hoernle, K., Hauff, F., Fiebig, J., 2006. Combined trace element and Pb-Nd-Sr-O isotope evidence for recycled oceanic crust (upper and lower) in the Iceland Mantle Plume. J. Petrol. 47 (9), 1705–1749. https://doi.org/10.1093/petrology/egl025.
- Lassiter, J., Hauri, E., 1998. Osmium-isotope variations in Hawaiian lavas: evidence for recycled oceanic lithosphere in the Hawaiian plume. Earth Planet. Sci. Lett. 164 (3–4), 483–496.
- Macpherson, C., Hilton, D., Day, J., Lowry, D., Gronvold, K., 2005. High-³He/⁴He, depleted mantle and low-δ¹⁸O, recycled oceanic lithosphere in the source of central Iceland magmatism. Earth Planet. Sci. Lett. 233 (3–4), 411–427. https://doi.org/10.1016/j.epsl.2005.02.037.
- Mundl-Petermeier, A., Walker, R., Jackson, M., Blichert-Toft, J., Kurz, M., Halldórsson, S.A., 2019. Temporal evolution of primordial tungsten-182 and ³He/⁴He signatures in the Iceland mantle plume. Chem. Geol. 525, 245–259.
- Neave, D.A., Putirka, K.D., 2017. A new clinopyroxene-liquid barometer, and implications for magma storage pressures under Icelandic rift zones. Am. Mineral. 102 (4), 777–794. https://doi.org/10.2138/am-2017-5968.
- Parnell-Turner, R., White, N., Henstock, T., Murton, B., Maclennan, J., Jones, S.M., 2014. A continuous 55-million-year record of transient mantle plume activity beneath Iceland. Nat. Geosci. 7 (12), 914–919. https://doi.org/10.1038/ngeo2281.
- Porcelli, D., Ballentine, C.J., 2002. Models for distribution of terrestrial noble gases and evolution of the atmosphere. Rev. Mineral. Geochem. 47 (1), 411–480.
- Rasmussen, M.B., Halldórsson, S.A., Gibson, S.A., Guðfinnsson, G.H., 2020. Olivine chemistry reveals compositional source heterogeneities within a tilted mantle plume beneath Iceland. Earth Planet. Sci. Lett. 531, 116008. https://doi.org/10. 1016/j.epsl.2019.116008.
- Shorttle, O., Maclennan, J., 2011. Compositional trends of Icelandic basalts: implications for short-length scale lithological heterogeneity in mantle plumes. Geochem. Geophys. Geosyst. 12 (11). https://doi.org/10.1029/2011gc003748.
- Sobolev, A.V., Hofmann, A.W., Kuzmin, D.V., Yaxley, C.M., Arndt, N.T., Chung, S.L., Danyushevsky, L.V., Elliott, T., Frey, F.A., Garcia, M.O., Gurenko, A.A., Kamenetsky, V.S., Kerr, A.C., Krivolutskaya, N.A., Matvienkov, V.V., Nikogosian, I.K., Rocholl, A., Sigurdsson, I.A., Sushchevskaya, N.M., Teklay, M., 2007. The amount of recycled crust in sources of mantle-derived melts. Science 316 (5823), 412–417. https://doi.org/10.1126/science, 1138113.
- Spice, H.E., Fitton, J.G., Kirstein, L.A., 2016. Temperature fluctuation of the Iceland mantle plume through time. Geochem. Geophys. Geosyst. 17 (2), 243–254.
- Starkey, N.A., Jackson, C.R.M., Greenwood, R.C., Parman, S., Franchi, I.A., Jackson, M., Fitton, J.G., Stuart, F.M., Kurz, M., Larsen, L.M., 2016. Triple oxygen isotopic composition of the high-³He/⁴He mantle. Geochim. Cosmochim. Acta 176, 227–238. https://doi.org/10.1016/j.gca.2015.12.027.
- Starkey, N.A., Stuart, F.M., Ellam, R.M., Fitton, J.G., Basu, S., Larsen, L.M., 2009. Helium isotopes in early Iceland plume picrites: constraints on the composition of high 3 He/ 4 He mantle. Earth Planet. Sci. Lett. 277 (1), 91–100.
- Sveinbjörnsdóttir, Á.E., Stefánsson, A., Heinemeier, J., Arnórsson, S., Eiríksdóttir, E.S., Ólafsdóttir, R., 2020. Assessing the sources of inorganic carbon in surface-, soil- and non-thermal groundwater in Iceland by δ^{13} C and 14 C. Geochim. Cosmochim. Acta.
- Thirlwall, M.F., Gee, M.A.M., Lowry, D., Mattey, D.P., Murton, B.J., Taylor, R.N., 2006. Low δ^{18} O in the Icelandic mantle and its origins: evidence from Reykjanes Ridge and Icelandic lavas. Geochim. Cosmochim. Acta 70 (4), 993–1019. https://doi.org/10.1016/j.gca.2005.09.008.
- Thirlwall, M.F., Gee, M.A.M., Taylor, R.N., Murton, B.J., 2004. Mantle components in Iceland and adjacent ridges investigated using double-spike Pb isotope ratios. Geochim. Cosmochim. Acta 68 (2), 361–386. https://doi.org/10.1016/s0016-7037(03)00424-1.
- Valley, J.W., Kitchen, N., Kohn, M.J., Niendorf, C.R., Spicuzza, M.J., 1995. UWG-2, a garnet standard for oxygen isotope ratios: strategies for high precision and accuracy with laser heating, Geochim. Cosmochim. Acta 59 (24), 5223–5231.
- Wessel, P., Smith, W.H.F., 1991. Free software helps map and display data. Eos 72 (41), 441–446. https://doi.org/10.1029/90eo00319.
- Willhite, L.N., Jackson, M.G., Blichert-Toft, J., Bindeman, I., Kurz, M.D., Halldórsson, S.A., Harðardóttir, S., Gazel, E., Price, A.A., Byerly, B.L., 2019. Hot and heterogenous high-³He/⁴He components: new constraints from proto-Iceland plume lavas from Baffin Island. Geochem. Geophys. Geosyst. 20 (12), 5939–5967. https://doi.org/10.1029/2019gc008654.
- Winpenny, B., Maclennan, J., 2014. Short length scale oxygen isotope heterogeneity in the Icelandic mantle: evidence from Plagioclase compositional zones. J. Petrol. 55 (12), 2537–2566. https://doi.org/10.1093/petrology/egu066.
- Workman, R.K., Eiler, J.M., Hart, S.R., Jackson, M.G., 2008. Oxygen isotopes in Samoan lavas: confirmation of continent recycling. Geology 36 (7), 551–554.
- Zakharov, D.O., Bindeman, I.N., Tanaka, R., Friðleifsson, G.Ó., Reed, M.H., Hampton, R.L., 2019. Triple oxygen isotope systematics as a tracer of fluids in the crust: a study from modern geothermal systems of Iceland. Chem. Geol. 530, 119312.